The Henryk Niewodniczański
INSTITUTE OF NUCLEAR PHYSICS
Polish Academy of Sciences
152 Radzikowskiego Str., 31-342 Kraków, Poland

www.ifj.edu.pl/reports/2005.html

Kraków, March 2005

REPORT No. 1961/PN

Preliminary study of a target-moderator assembly for a linac-based neutron source

Sergio Bartalucci[1)], *Krzysztof Drozdowicz,*
Dominik Dworak, Grzegorz Tracz, Vladimir Angelov[2)]

[1)] Istituto Nazionale di Fisica Nucleare, Laboratori Nazionali di Frascati
via Enrico Fermi 40, I-00044 Frascati (Roma), Italy

[2)] Institute for Nuclear Research and Nuclear Energy
72 Tzarigradsko chaussee blvd, BG-1784 Sofia, Bulgaria

The work has been partly sponsored by the TARI LNF funding
under Contract No.RII3-CT-2004-506078, Project NEUTSO1.

Abstract

The report concerns a design of a future pulsed neutron source at an electron linac. A massive target is irradiated with an electron beam and the neutrons are generated mainly by collisions of the bremsstrahlung photons. A first step of the work, related to the optimization of the target materials and geometry using numerical simulations, is presented. The Monte Carlo FLUKA and MCNP codes are used. The water-cooled tantalum target is investigated: 0.41 cm Ta slices separated with 0.15 cm H_2O layers. Two different sizes of the cylindrical target are assumed: 5 or 2.5 cm in diameter. The 1 GeV and 1.5 GeV electron beams are tested. The outgoing neutron angular-energy spectra are presented. The angular space 0°÷180° is divided in 10-degree intervals. The neutron emission in the direction perpendicular

to the originated electron beam has been observed in the particularly narrow (2°) interval. The FLUKA results of a comparison of the neutron currents in main directions (0° – forward, 90° – perpendicular, 180° – backward) are as follows. For the 5 cm target the distribution is quite uniform: at 1 GeV input electrons – $n(180°)/n(0°) = 1.00$, $n(90°)/n(0°) = 1.04$, and at 1.5 GeV electrons – $n(180°)/n(0°) = 0.91$, $n(90°)/n(0°) = 1.00$. For the 2.5 cm target the relative neutron current in the perpendicular direction is significantly higher: at 1 GeV electrons – $n(180°)/n(0°) = 1.02$, $n(90°)/n(0°) = 1.53$, and at 1.5 GeV electrons – $n(180°)/n(0°) = 0.93$, $n(90°)/n(0°) = 1.45$. In the cases when the FLUKA and MCNP simulation results can be compared, a high similarity of the neutron energy distributions is stated although a possible discrepancy of the values reaches 20 %. Spectra of the accompanying radiation (photons, electrons, positrons, protons, charged pions) have been also obtained. The angular distributions of photons, electrons, and positrons are strongly peaked up towards the beam direction. Their emission at 90° is significantly lower, which means a decrease of the background in this direction. The energy deposition in the target is estimated on a simplified model with no cooling system. About 63 % of energy is then stored in the space at ca. 20÷40 % target length along the initial electron beam axis.

1. Introduction

The accelerator-based neutron source has certain important advantages in comparison to another types of sources (like nuclear reactors or radioisotope neutron emiters). It can produce short bursts of neutrons with a broad continuous energy spectrum by nuclear reactions of energetic photons or charged particles. Especially, a linac is a powerful tool to produce intense pulsed neutron beams. Pulsed neutrons based on an electron linac are effective for measuring energy-dependent cross-sections with high resolution by the time-of-flight (TOF) technique covering the energy range from thermal neutrons to a few tens of MeV. Precise measurements of the neutron-cross sections are of great importance for the safety design of nuclear reactors and for the evaluation of the neutron flux density and energy spectrum around a reactor. Fusion reactors are another example, where the interactions of neutron and photon fields from D–T fusion with the surrounding medium (first wall, blanket, and vacuum vessel) are still poorly known.

The neutron source is modelled as a final product of the electron beam, which hits a massive target material (a high atomic number, Z). In this manner neutrons are produced inside the target mainly by the inelastic collisions of the bremsstrahlung photons.

This report presents a part of the joint work ongoing at the Laboratori Nazionali di Frascati, LNF (of the Instituto Nazionale di Fisica Nucleare, INFN, Italy), and the Dept. of the Environmental and Radiation Transport Physics of the Institute of Nuclear Physics, Polish Academy of Sciences (IFJ PAN, Poland). The main effort of this collaboration is focused on numerical optimization of the target-moderator assembly in order to get an intense, well-defined final neutron beam. The project concerns a design of the neutron source at an electron linac to be built in the Rome Research Area. A deeper information on the project can be found in papers by Alesini *et al.* (2003a, 2003b) and Bartalucci *et al.*, (2004). The Beam Test Facility (Mazzitelli and Valente, 2003) at the existing DAΦNE Linac is intended to be used later for tests of the photoneutron source.

The neutron output from a cylindrical tantalum target is studied using Monte Carlo simulations of the developing electro-magnetic and hadron cascades. Two different energies of the incident electrons are considered. The geometry assumed for the simulations is shown in Fig 1. The cylindrical target is not uniform. It consists of ten tantalum plates, each one of 0.41 cm in thickness. Thin layers of water (each 0.15 cm thick) are modelled between the tantalum plates as the cooling system for the target. The target diameter has been assumed in most calculations to 5 cm, although a smaller one (2.5) has been also tried. The emitted

particles are scored on the surface of a sphere, which surrounds the target positioned at its center. The sphere radius R is arbitrary (It has been set to 1 or 10 m, depending on the simulated case).

Fig. 1. Geometry assumed for the MC simulations.

2. Calculations

The calculations have been performed using the Monte Carlo codes, FLUKA and MCNP (Briesmaister, 2000). The latest available versions have been used: FLUKA-2003 (Fasso *et al*., 2003) and the MCNP5 (X-5, 2003). Beside of the main subject (the final neutron yield), spectra of outgoing charged hadrons, photons and electrons have been also calculated for further purposes in connection to radiation protection problems of the proposed design. The calculations by means of both codes (MCNP and FLUKA) have been performed for the target diameter equal to 5 cm and the primary beam energy equal to 1 GeV. The neutron yields and energy spectra are determined in two narrow ϑ angle ranges: 89 ÷ 91 deg and 89.9 ÷ 90.1 deg,

that means perpendicularly to the primary electron beam direction (see Fig.1). A comparison of the results is given in paragraph 3.

Other results presented in the report (as well for neutrons as charged particles and photons) have been obtained by use of the FLUKA code only (Fasso *et al.*, 2001a, 2001b). Calculations for another diameter of the target (2.5 cm) have been also performed in order to investigate an influence of the target size on the yields and spectra of the produced neutrons.

The sliced tantalum-water target is irradiated by the pencil-like one-dimensional electron beam. The incident electron energy is assumed to 1.0 or 1.5 GeV. Unfortunately, the MCNP code does not allow to carry on simulations for electrons and photons of energies higher than 1 GeV. Therefore, calculations above this energy could be performed only by means of the FLUKA code. The essential results are presented in this report. Other detailed data, like double differential angular-energy distributions of all produced particles, for the four considered combinations of the primary beam energies and target dimensions, are available from the authors.

The angular spectra have been calculated in the following ϑ angle bins (in degrees): (0 ÷ 10), (10 ÷ 20), (20 ÷ 30), (30 ÷ 40), (40 ÷ 50), (50 ÷ 60), (60 ÷ 70), (70 ÷ 80), (80 ÷ 89), (89 ÷ 91), (91 ÷ 100), (100 ÷ 110), (110 ÷ 120), (120 ÷ 130), (130 ÷ 140), (140 ÷ 150), (150 ÷ 160), (160 ÷ 170), and (170 ÷ 180). A special case of the very narrow angular bin (89.9 ÷ 90.1) deg has been treated separately. The following particles have been tracked: neutrons, protons, charged pions, photons, electrons, and positrons. The so-called boundary crossing one-way estimator has been applied to score the particle currents. In the Monte Carlo slang this expression means that each particle is scored when it crosses the given surface (called sometimes the detector surface). Here, all particles have been scored on the surface of the sphere, which surrounds the target positioned at its center. The whole sphere has been divided into 19 detectors – spherical rings, limited by two polar ϑ angles according to the angular ranges defined above. When any particle crosses the given detector it is considered as emitted into the corresponding angular range (the point source approximation). This approximation is adequate when the ratio of the radius R to the target size is high and allows to study the particle field around the target. The sphere radius R has been arbitrarily set to 100 cm. Only in the case of the mentioned very narrow ϑ angle range (89.9 to 90.1 deg) the produced particles have been counted on the sphere at R = 1000 cm.

Hadrons are produced mainly by the bremsstrahlung photons. Four types of the photonuclear interactions producing hadrons are taken into account in the present FLUKA

version :

– production via Giant Dipole Resonance interactions,

– production via quasi-deuteron interactions,

– production in the region of the Delta resonance,

– other high-energy interactions (above 0.7 GeV).

They can be treated separately, switched on or off. In the present calculations all of these possible reactions have been switched on.

The following energy cut-off values (energy thresholds) for the particle transport inside the target have been used:

– neutrons: 10^{-5} eV

– protons: 1 MeV

– π^+, π^-: 1 MeV

– photons: 10 keV

– e^+, e^-: 100 keV

other particles: 10 MeV.

Interactions and transport of neutrinos and heavy ions are not included into the calculations.

3. Angular and energy spectra

The neutron current has been calculated at the distance R = 1 m from the target (two different diameters, 5 cm and 2.5 cm, and two primary beam energies, 1 GeV and 1.5 GeV). The dependence of the neutron current on the emission angle ϑ and neutron energy E is tabulated in the Appendix (Tables A1.1 to A1.4). The angular distribution of the relative neutron current in the most important energy intervals is plotted in Fig. 2.

In the case of a larger target (5 cm in diameter) and neutron energies below 10 MeV the angular distributions are almost independent of the ϑ angle. A weak and broad maximum of the neutron current can be observed in the direction perpendicular to the beam axis (near ϑ = 90 deg). For higher neutron energies, above 10 MeV, the angular distribution shows an evident increase for low ϑ values, *i.e.* towards the flight of primary electrons. However, the total neutron flux is dominated by low-energy neutrons (below 10 MeV), so these differences disappear when one looks at the angular distribution of all emitted neutrons (the last column in Tables A1.1 to A1.4).

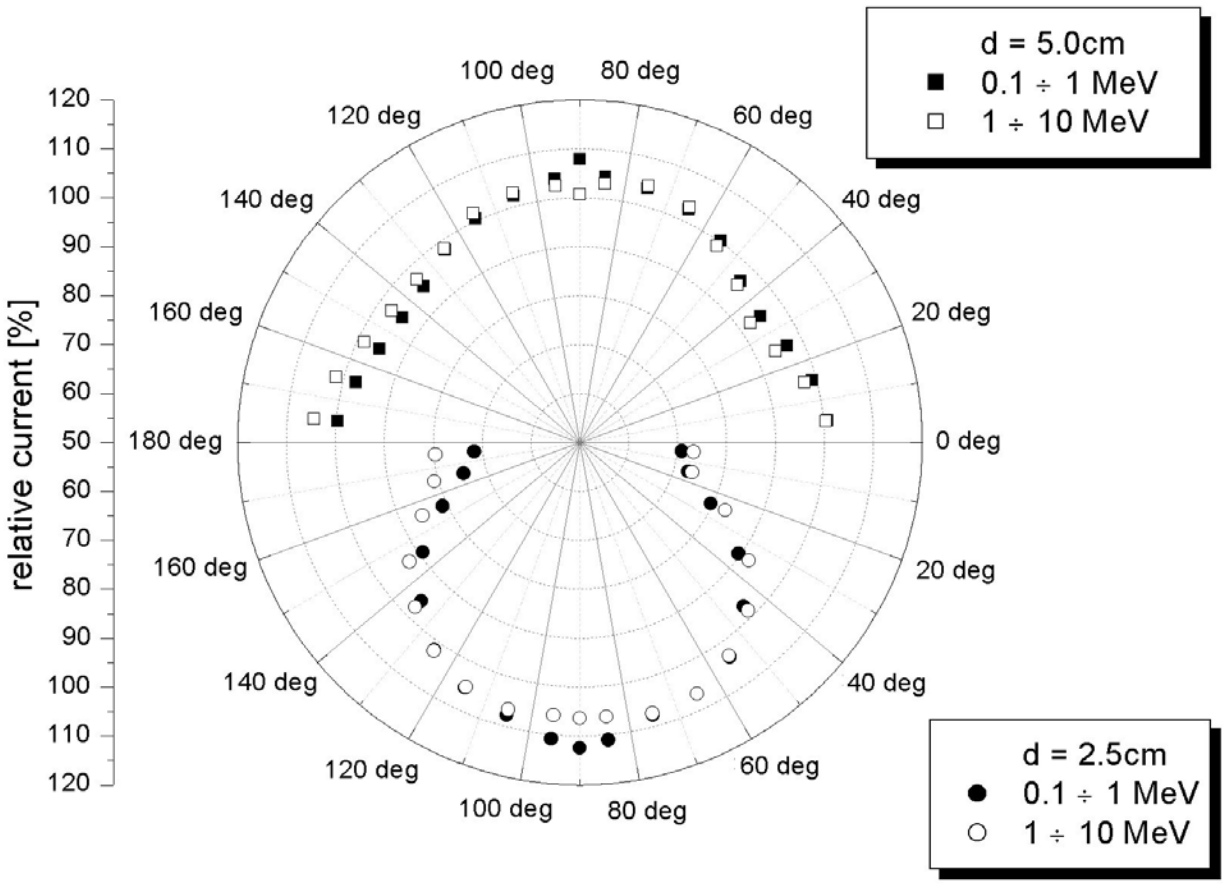

Fig. 2. Angular distribution of the relative neutron current at R = 1 m from the targets of 2.5 and 5 cm in diameter.

For a smaller target (diameter d = 2.5 cm) and low energy neutrons, the broad maximum at $\vartheta \approx 90$ deg is much stronger. The number of neutrons emitted perpendicularly to the beam direction is higher roughly by a factor of two than of those emitted forward or backward (the low or high ϑ angles). A smaller diameter of the target means a higher transparency for neutrons emitted in the direction perpendicular to the target axis. Thus, one can observe more outgoing neutrons. Additionally, the number of neutron collisions inside the target is reduced and the observed neutron spectrum is a bit harder (see Fig. 4b).

It is interesting that in both cases (d = 5 or 2.5 cm) the total neutron fluxes are almost the same: $2.70 \cdot 10^{-6}$ n/cm^2/b.part. in the first case, against $2.64 \cdot 10^{-6}$ n/cm^2/b.part. in the other one. Only the angular flux distributions for low-energy neutrons behave differently.

The increase of the primary beam energy from 1 GeV to 1.5 GeV manifests mainly in higher neutron yields (compare data in Tables A1.1 with A1.3 and A1.2 with A1.4). The shapes of the neutron angular distributions and energy spectra seem to be very similar in both cases. While comparing the corresponding neutron currents one can find that the number of

produced neutrons in the case of 1.5 GeV electron beam is roughly 50% higher. Thus, one can expect that in this energy range, between 1.0 and 1.5 GeV, the total neutron production increases linearly with the electron beam energy.

Values of the currents of other produced particles are presented in Table A2 in the Appendix. The data are shown only for one case: the target diameter d = 5 cm and the electron beam energy equal to 1 GeV. As one could expect, the angular distributions of photons, electrons, and positrons are strongly peaked up towards the beam direction. Behaviour of protons and charged pions has been found interesting. Their angular distributions are peaked up forward and backward as well, with evident broad minimum in the direction perpendicular to the beam axis. These results are not obvious and one can suppose that at a high energy (over 150 MeV) they depend on the actual Intranuclear Cascade models, which are used in the computer codes used. The authors hope to explain this in the nearest future.

The neutron yields and energy spectra in the direction perpendicular to the beam direction have been particularly carefully investigated by means of both used codes, FLUKA and MCNP, for the 1 GeV electrons irradiating the target d = 5 cm. A comparison of the results is presented in Fig. 3. The calculations have been made in two variants: (i) neutrons have been scored at the distance R = 1 m from the target centre at the ϑ angle between 89 and 91 deg, Fig. 3a, and (ii) within the very narrow ϑ interval, 89.9 to 90.1 deg, at R = 10 m, Fig 3b.

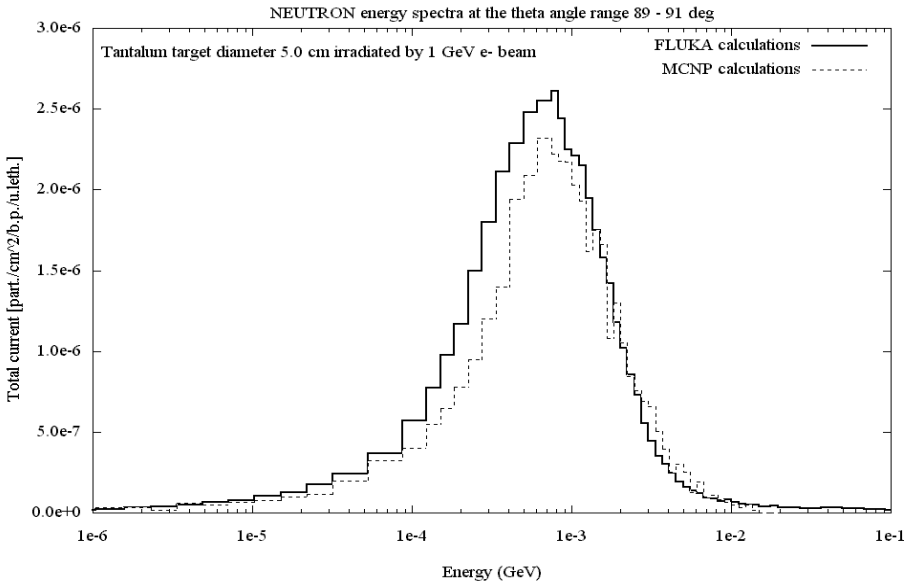

Fig. 3a. Spectra of neutrons emitted perpendicularly to the beam direction, 89 deg < ϑ < 91 deg. Comparison of the FLUKA and MCNP simulations.

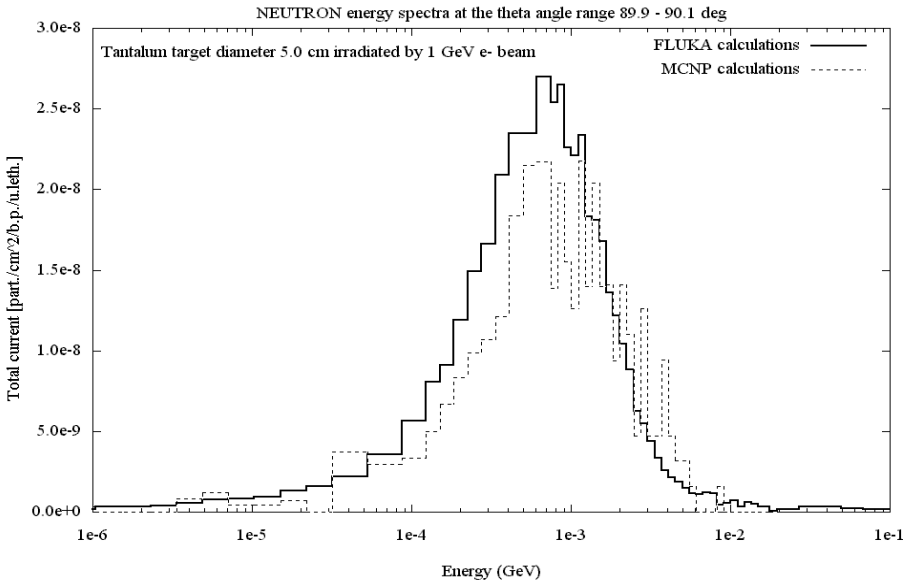

Fig. 3b. Spectra of neutrons emitted perpendicularly to the beam direction in a very narrow ϑ range, 89.9 deg < ϑ < 90.1 deg. Comparison of the FLUKA and MCNP simulations.

The spectra in Fig. 3b (a narrow ϑ range) obtained from both codes are a little bit shifted towards lower energies in comparison to the spectra in Fig. 3a (a wider ϑ range). A comparison of the FLUKA and MCNP results shows that the MCNP code produces a little more energetic neutrons. The total number of produced neutrons is higher in the case of the FLUKA simulations. The corresponding absolute values, in neutrons/cm^2/beam particle, are: $2.82 \cdot 10^{-6}$ (FLUKA) against $2.37 \cdot 10^{-6}$ (MCNP) at a wider ϑ range, and $2.81 \cdot 10^{-8}$ (FLUKA) against $2.26 \cdot 10^{-8}$ (MCNP) at the narrow ϑ range. These differences are too high to be explained by the fact that the MCNP cross-section libraries for neutrons are limited to 150 MeV (or even only 20 MeV for some elements). The FLUKA simulates high-energy neutrons and the energy spectrum tail extends up to 400 MeV (or even up to 800 MeV in the case of the forward neutrons at ϑ below 10 deg) but this amount is almost negligible. An irregular shape of the MCNP-produced spectrum above 1 MeV in Fig. 3b reflects rather statistical fluctuations than a physical effect. This is not visible in the corresponding spectrum at a wider angle (Fig. 3a).

Characteristics of the neutron output from the target for other conditions have been investigated only by FLUKA simulations. The dependence of the neutron energy spectra on the primary beam energy, target diameter, and neutron emission angle is presented in Figs. 4a,

4b, 4c. Four curves for different beam energies (1 GeV or 1.5 GeV) and target diameters (5 cm or 2.5 cm) are plotted in each figure. Three most characteristic neutron emission angle ranges are chosen to be presented: forward ($\vartheta < 10$ deg) in Fig. 4a, perpendicular (89 deg < ϑ < 91 deg) in Fig. 4b, and backward (ϑ >170) in Fig. 4c. Looking at these figures one can conclude that all the curves are very similar. That means, shapes of the energy distributions of produced neutrons are almost independent not only of the beam energy and target diameter but also of the emission angle. The absolute values of the corresponding particular currents are different and behave according to the expectations mentioned earlier.

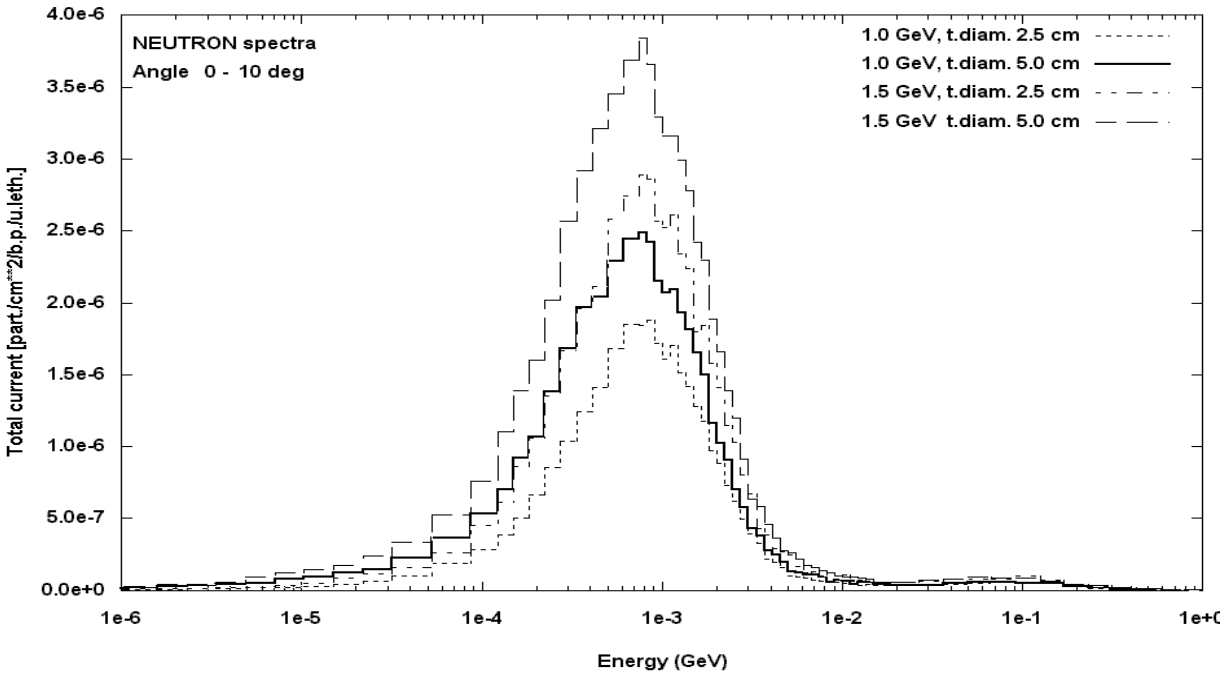

Fig. 4a. Neutron energy spectra at $0 < \vartheta < 10$ deg.

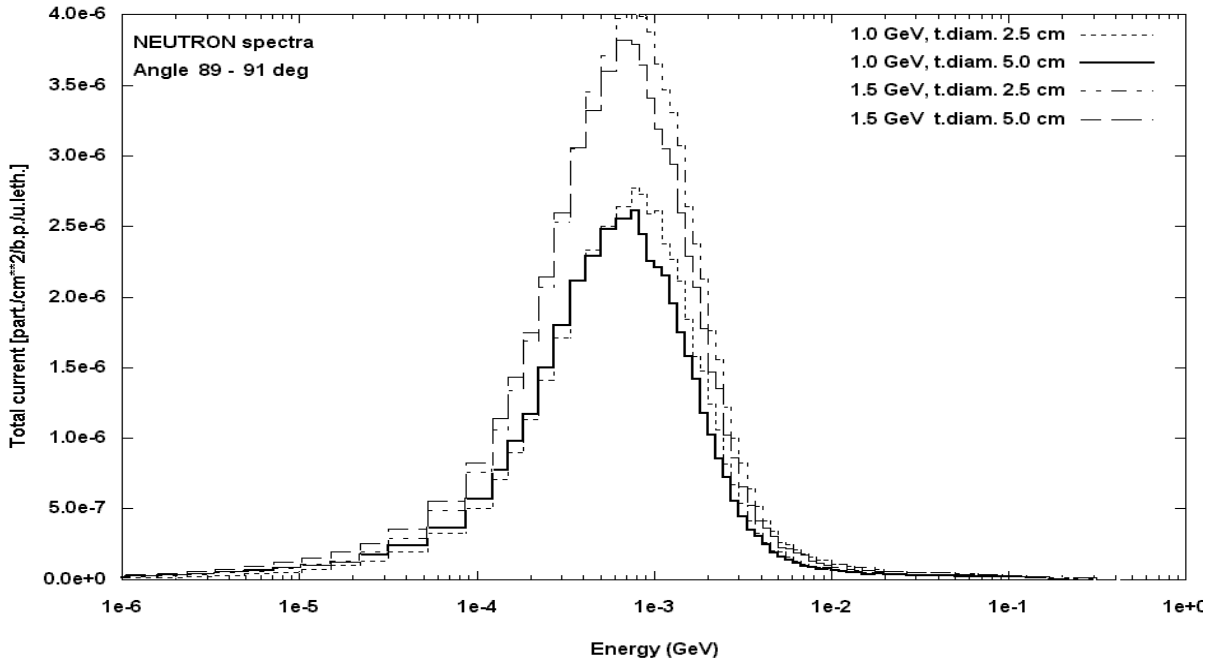

Fig. 4b. Neutron energy spectra at $89 < \vartheta < 91$ deg.

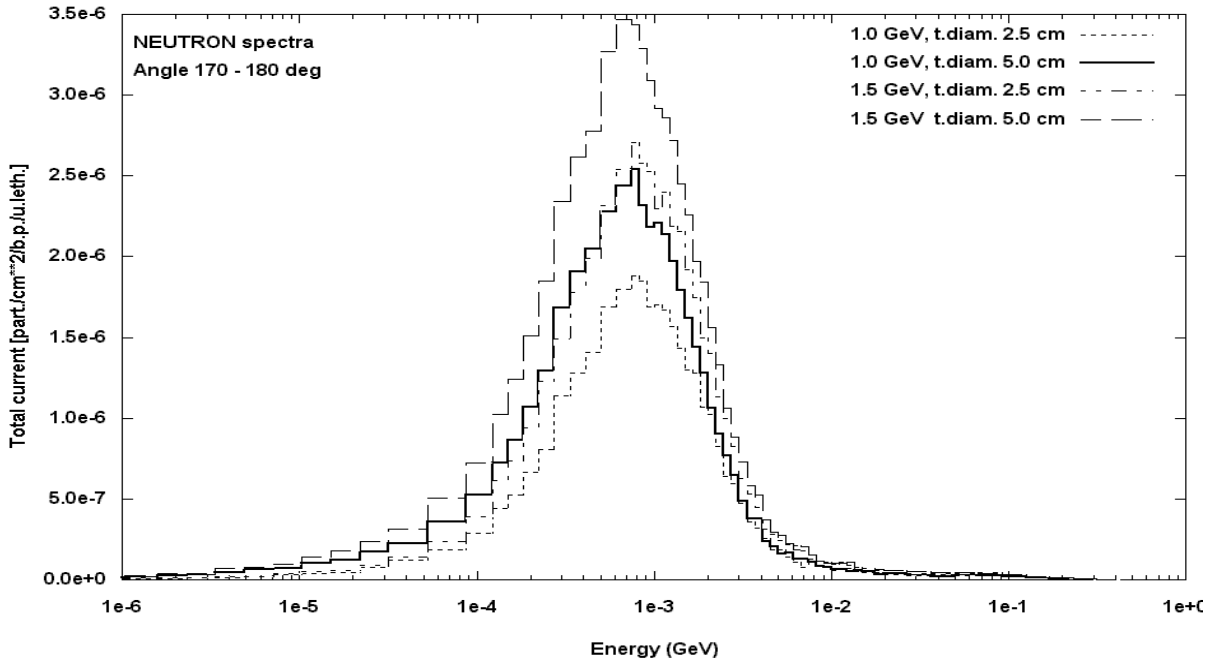

Fig. 4c. Neutron energy spectra at $170 < \vartheta < 180$ deg.

Energy spectra of other particles, emitted from the tantalum target of 5 cm diameter, irradiated by 1 GeV electrons, are shown in the Appendix in Figs. A3.1–A3.5. (protons, charged pions, photons, electrons, positrons). Three curves are plotted in each figure – emission at different ϑ angles: $\vartheta < 10$ deg, $40 < \vartheta < 50$ deg, and $80 < \vartheta < 89$ deg. The spectra are normalized to unity and, thus, their shapes at different angle ranges can be directly compared (The absolute values are given in Table A2). The results are in agreement with expectations: when the emission angle is higher then the corresponding energy spectrum is shifted towards lower energies. The highest differences are observed for photons. The photon spectrum at low ϑ angles (below 10 deg) is totally dominated by photons originated directly from the development of the electromagnetic cascades. Opposite to that, photons at higher ϑ angles originate mainly from inelastic collisions of the low-energy neutrons with the tantalum nuclei, neutron capture, and deexcitations of the nuclei.

4. Energy deposition in the target

A simplified case has been simulated using the MCNP code in order to estimate how energy of incident electrons is deposited in the target. The energy of the electron beam has been set to 1 GeV. The target has been assumed as tantalum of 4.1 cm thickness (10 radiation lengths for this material) and 5 cm diameter with no cooling system. The target has been divided into 100 cells, in which the deposited energy has been tallied: 10 slices of 0.41 cm each in the longitudinal direction (*i.e.* along the z-axis) and 10 slices with increment of 0.25 cm in the vertical direction (*i.e.* along the target radius). Since the cells are not equal in volume (and mass) the results has been normalized per one cubic centimetre.

Fig. 5 presents the calculated distribution of the deposited energy. The majority of energy (about 63 % when not normalized per volume unit) is stored in the z-axis region with the maximum between 0.8 and 1.6 cm. Other 20 % of energy (also non-normalized) is deposited in the next zone with regard to radius (between 0.25 and 0.50 cm). The farther from the z-axis the more the maximum is shifted toward the target rear, and less energy is stored. However, the more important quantity is energy put up per volume (or mass) unit. The centre of the target appears to be most important region. Other sections are of a much lesser importance.

The foregoing case, when the target is homogenous, although very simple is instructive. The deposition of energy in more complex cases will be investigated in future.

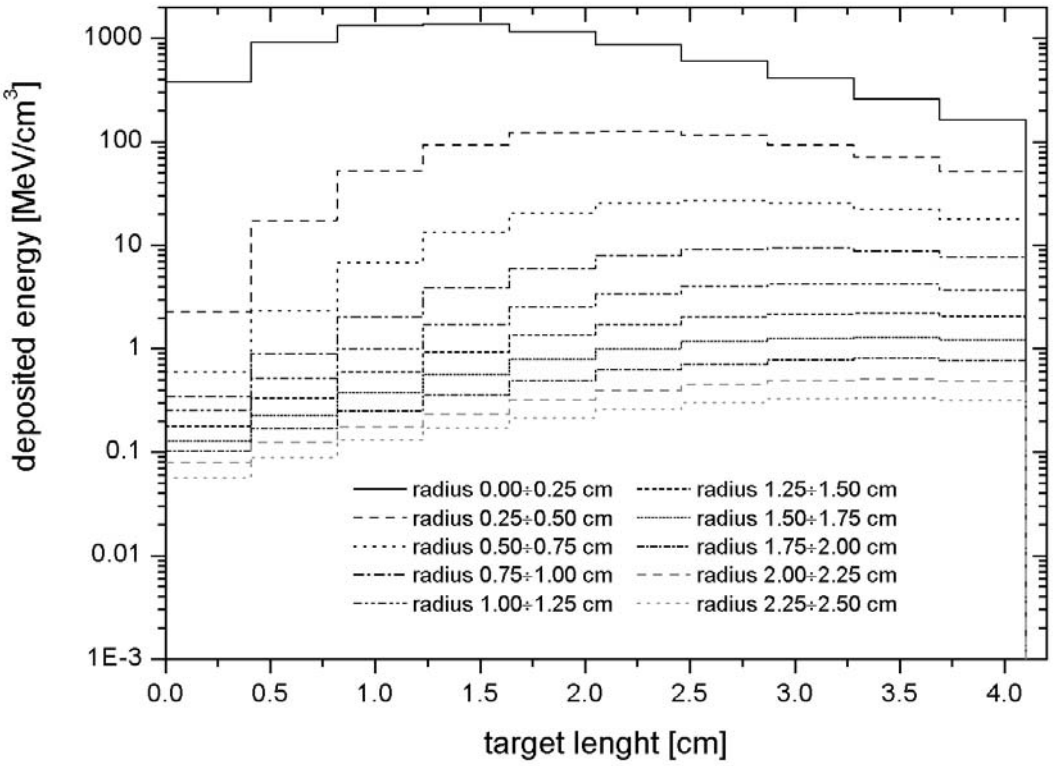

Fig. 5. Energy deposited in the tantalum target of the 4.1 cm thickness and 5 cm diameter. Energy of incident electrons is 1 GeV.

5. Conclusions

The presented results are not a complete study of the optimization of the target for the neutron source based on an electron linac. They can be considered as a preliminary part of the work. The configuration of the target (the material as well as the cooling medium and the geometry) can be different. Here, two incident electron energies and two diameters of the same cylindrical target have been assumed. The neutron output in the direction perpendicular to the incident electron been has been particularly studied. The emission of other particles (creating the background) in this direction is significantly lower than forward. The total neutron current from the 5-cm-diameter target is almost independent on the emission angle. In the case of a smaller target (2.5 cm) the forward and backward neutron currents are lower but the perpendicular one is still on the same level.

The results obtained from the MCNP and FLUKA simulations (in the cases when this is

possible) are similar. The discrepancy is on the level of about 20 %.

A relative approximate distribution of the energy deposition has been obtained in the target which is not cooled. The absolute values are available when the intensity of the initial electron beam is assumed.

The work is continued.

Acknowledgment

This research is a part of the EU Integrated Infrastructure Initiative HadronPhysics Project under contract number RII3-CT-2004-506078, Project NEUTSO1.

References

Alesini D. *et al.* (2003a)
Conceptual design of a high-brightness linac for soft X-ray SASE-FEL source.
Nucl. Instrum. Meth. **A 507,** 502–506.

Alesini D. *et al.* (2003b)
The SPARC project: a high-brightness electron beam source at LNF to drive a SASE-FEL experiment
Nucl. Instrum. Meth. **A 507**, 345–349.

Bartalucci S., Angelov V., Drozdowicz K., Tracz G. (2004)
A linac-based neutron source for time-of-light (TOF) measurements.
SATIF-7 *Shielding Aspects of Accelerators, Targets and Irradiation Facilities, Seventh Meeting 17-18 May 2004,* Sacavem (Lisbon), Portugal [in print].

Briesmaister J.F. (2000)
MCNP – A General Monte Carlo N-Particle Transport Code. Version4C.
LA-13709-M, Los Alamos National Laboratory.

Fasso A., Ferrari A., Sala P.R. (2001a)
Electron-photon transport in FLUKA: Status.
Proc. of the Monte Carlo 2000 Conference on "Advanced Monte Carlo for Radiation Physics, Particle Transport Simulation and Application", Lisbon 23-26 October 2000.
A.King et al. (Eds), Springer, Berlin, pp. 159-164.

Fasso A., Ferrari A., Ranft J., Sala P.R. (2001b)
FLUKA: Status and Prospective for Hadronic Applications.
Proc. of the Monte Carlo 2000 Conference on "Advanced Monte Carlo for Radiation Physics, Particle Transport Simulation and Application", Lisbon 23-26 October 2000.
A.King et al. (Eds), Springer, Berlin, pp. 955-960.

Fasso A., Ferrari A., Ranft J., Sala P.R. (2003)
FLUKA-2003 Manual.
www.fluka.org

Mazzitelli G., Valente P. (2003)
Commissioning of the DAFNE Beam Test Facility.
LNF-03/003(P), Frascati.

X-5 Monte Carlo Team (2003)
MCNP – A General Monte Carlo N-Particle Transport Code. Version 5.
LA-UR-03-1987, Los Alamos National Laboratory.

Appendixes

A1. Tables of the dependence of the neutron current on the emission angle and energy.

A2. Table of the dependence of the currents of other particles on the emission angle.

A3. Plots of the energy spectra of the particles emitted at various angles.

Table A1.1. Neutron current at $R = 1$ m from the target (see Fig. 1)

(in neutrons/cm^2/one beam electron)

Target diameter: **5** cm, Energy of the electron beam: **1.0** GeV

Total number of beam particles followed by FLUKA: 300000

	Neutron energy ranges				
Angle range	E<100 keV	100keV-1MeV	1MeV-10MeV	E>10 MeV	All
0 - 10 deg	2.60E-07	1.61E-06	7.68E-07	6.70E-08	2.71E-06
10 - 20 deg	2.70E-07	1.59E-06	7.46E-07	6.31E-08	2.67E-06
20 - 30 deg	2.74E-07	1.55E-06	7.20E-07	5.43E-08	2.60E-06
30 - 40 deg	2.79E-07	1.52E-06	7.08E-07	5.08E-08	2.56E-06
40 - 50 deg	2.89E-07	1.55E-06	7.31E-07	4.89E-08	2.61E-06
50 - 60 deg	2.99E-07	1.61E-06	7.56E-07	4.72E-08	2.71E-06
60 - 70 deg	3.07E-07	1.64E-06	7.88E-07	4.43E-08	2.78E-06
70 - 80 deg	3.12E-07	1.66E-06	7.97E-07	4.17E-08	2.81E-06
80 - 89 deg	3.01E-07	1.67E-06	7.88E-07	3.87E-08	2.80E-06
89 - 91 deg	2.84E-07	1.73E-06	7.70E-07	3.61E-08	2.82E-06
91 - 100 deg	3.00E-07	1.67E-06	7.85E-07	3.64E-08	2.79E-06
100 - 110 deg	3.10E-07	1.64E-06	7.85E-07	3.68E-08	2.77E-06
110 - 120 deg	3.04E-07	1.61E-06	7.77E-07	3.68E-08	2.73E-06
120 - 130 deg	2.96E-07	1.57E-06	7.52E-07	3.63E-08	2.66E-06
130 - 140 deg	2.87E-07	1.52E-06	7.42E-07	3.67E-08	2.59E-06
140 - 150 deg	2.78E-07	1.51E-06	7.41E-07	3.68E-08	2.57E-06
150 - 160 deg	2.72E-07	1.52E-06	7.54E-07	3.73E-08	2.59E-06
160 - 170 deg	2.67E-07	1.56E-06	7.76E-07	3.81E-08	2.64E-06
170 - 180 deg	2.63E-07	1.60E-06	7.99E-07	3.69E-08	2.70E-06
Full range:					
0 - 180 deg	2.95E-07	1.60E-06	7.65E-07	4.16E-08	2.70E-06

Neutron current relative to the corresponding averages included in the row "Full range: 0-180 deg" (in per cent)

Angle range	E<100 keV	100keV-1MeV	1MeV-10MeV	E>10 MeV	All
0 - 10 deg	88.44	100.79	100.48	161.21	100.29
10 - 20 deg	91.69	99.11	97.60	151.68	98.68
20 - 30 deg	92.93	96.70	94.15	130.56	96.09
30 - 40 deg	94.60	94.95	92.64	122.32	94.68
40 - 50 deg	98.02	96.51	95.61	117.73	96.75
50 - 60 deg	101.45	100.29	98.89	113.56	100.22
60 - 70 deg	104.35	102.57	103.10	106.57	102.98
70 - 80 deg	105.89	103.77	104.20	100.25	104.07
80 - 89 deg	102.28	104.52	103.06	93.00	103.68
89 - 91 deg	96.26	107.86	100.68	86.81	104.24
91 - 100 deg	101.77	104.07	102.66	87.59	103.17
100 - 110 deg	105.22	102.18	102.74	88.44	102.46
110 - 120 deg	103.33	100.40	101.59	88.60	100.88
120 - 130 deg	100.44	98.06	98.37	87.37	98.24
130 - 140 deg	97.52	95.14	97.10	88.27	95.85
140 - 150 deg	94.54	94.32	96.94	88.41	95.00
150 - 160 deg	92.45	95.16	98.61	89.74	95.76
160 - 170 deg	90.50	97.39	101.54	91.71	97.73
170 - 180 deg	89.27	99.63	104.55	88.86	99.72
0 - 180 deg	100.00	100.00	100.00	100.00	100.00

Table A1.2. Neutron current at R = 1 m from the target (see Fig. 1)

(in neutrons/cm^2/one beam electron)

Target diameter: **2.5** cm, Energy of the electron beam: **1.0** GeV

Total number of beam particles followed by FLUKA: 200000

	Neutrons				
Angle range	E<100 keV	100keV-1MeV	1MeV-10MeV	E>10 MeV	All
0 - 10 deg	1.11E-07	1.10E-06	6.20E-07	6.53E-08	1.90E-06
10 - 20 deg	1.27E-07	1.13E-06	6.24E-07	5.80E-08	1.94E-06
20 - 30 deg	1.44E-07	1.23E-06	7.00E-07	6.11E-08	2.14E-06
30 - 40 deg	1.67E-07	1.39E-06	7.79E-07	6.01E-08	2.39E-06
40 - 50 deg	1.94E-07	1.51E-06	8.34E-07	5.48E-08	2.59E-06
50 - 60 deg	2.11E-07	1.60E-06	8.73E-07	5.14E-08	2.74E-06
60 - 70 deg	2.24E-07	1.65E-06	9.02E-07	4.68E-08	2.82E-06
70 - 80 deg	2.29E-07	1.67E-06	9.08E-07	4.44E-08	2.85E-06
80 - 89 deg	2.31E-07	1.72E-06	8.99E-07	4.21E-08	2.89E-06
89 - 91 deg	2.25E-07	1.74E-06	8.99E-07	3.98E-08	2.90E-06
91 - 100 deg	2.30E-07	1.72E-06	8.96E-07	3.94E-08	2.88E-06
100 - 110 deg	2.28E-07	1.67E-06	9.00E-07	3.83E-08	2.83E-06
110 - 120 deg	2.24E-07	1.63E-06	8.89E-07	3.85E-08	2.78E-06
120 - 130 deg	2.09E-07	1.58E-06	8.62E-07	3.80E-08	2.69E-06
130 - 140 deg	1.90E-07	1.48E-06	8.25E-07	3.67E-08	2.53E-06
140 - 150 deg	1.68E-07	1.38E-06	7.82E-07	3.60E-08	2.37E-06
150 - 160 deg	1.43E-07	1.25E-06	7.23E-07	3.64E-08	2.15E-06
160 - 170 deg	1.30E-07	1.15E-06	6.83E-07	3.54E-08	2.00E-06
170 - 180 deg	1.21E-07	1.11E-06	6.73E-07	3.78E-08	1.94E-06
Full range:					
0 - 180 deg	2.02E-07	1.55E-06	8.45E-07	4.41E-08	2.64E-06

Neutron current relative to the corresponding averages included in the row "Full range: 0-180 deg" (in per cent)

Angle range	E<100 keV	100keV-1MeV	1MeV-10MeV	E>10 MeV	All
0 - 10 deg	55.08	70.98	73.34	148.29	71.81
10 - 20 deg	62.78	72.99	73.79	131.65	73.45
20 - 30 deg	71.27	79.57	82.81	138.58	80.95
30 - 40 deg	82.67	89.64	92.17	136.29	90.70
40 - 50 deg	95.87	97.33	98.62	124.34	98.08
50 - 60 deg	104.22	103.51	103.24	116.70	103.70
60 - 70 deg	110.64	106.74	106.68	106.13	107.01
70 - 80 deg	113.29	107.63	107.35	100.75	107.86
80 - 89 deg	113.96	111.08	106.33	95.64	109.52
89 - 91 deg	111.45	112.40	106.35	90.29	110.02
91 - 100 deg	113.59	110.87	106.04	89.43	109.17
100 - 110 deg	112.60	107.68	106.51	86.90	107.34
110 - 120 deg	110.95	105.36	105.15	87.31	105.42
120 - 130 deg	103.34	101.85	101.99	86.18	101.74
130 - 140 deg	93.95	95.83	97.59	83.30	96.04
140 - 150 deg	83.21	89.11	92.51	81.76	89.62
150 - 160 deg	70.53	80.95	85.48	82.69	81.63
160 - 170 deg	64.07	74.54	80.74	80.37	75.82
170 - 180 deg	59.70	71.66	79.60	85.75	73.52
0 - 180 deg	100.00	100.00	100.00	100.00	100.00

Table A1.3. Neutron current at R = 1 m from the target (see Fig. 1)

(in neutrons/cm^2/one beam electron)

Target diameter: **5** cm, Energy of the electron beam: **1.5** GeV
Total number of beam particles followed by FLUKA: 200000

	Neutrons				
Angle range	E<100 keV	100keV-1MeV	1MeV-10MeV	E>10 MeV	All
0 - 10 deg	3.91E-07	2.44E-06	1.19E-06	1.09E-07	4.14E-06
10 - 20 deg	3.99E-07	2.40E-06	1.15E-06	1.06E-07	4.05E-06
20 - 30 deg	4.13E-07	2.34E-06	1.10E-06	9.37E-08	3.95E-06
30 - 40 deg	4.18E-07	2.30E-06	1.08E-06	8.31E-08	3.88E-06
40 - 50 deg	4.28E-07	2.31E-06	1.09E-06	8.09E-08	3.92E-06
50 - 60 deg	4.40E-07	2.39E-06	1.14E-06	7.72E-08	4.05E-06
60 - 70 deg	4.51E-07	2.42E-06	1.18E-06	7.29E-08	4.12E-06
70 - 80 deg	4.57E-07	2.44E-06	1.18E-06	6.92E-08	4.15E-06
80 - 89 deg	4.39E-07	2.46E-06	1.16E-06	6.49E-08	4.13E-06
89 - 91 deg	4.25E-07	2.53E-06	1.13E-06	5.99E-08	4.15E-06
91 - 100 deg	4.38E-07	2.43E-06	1.15E-06	6.02E-08	4.08E-06
100 - 110 deg	4.50E-07	2.38E-06	1.16E-06	6.04E-08	4.05E-06
110 - 120 deg	4.42E-07	2.34E-06	1.14E-06	5.97E-08	3.98E-06
120 - 130 deg	4.26E-07	2.27E-06	1.11E-06	5.83E-08	3.86E-06
130 - 140 deg	4.11E-07	2.17E-06	1.08E-06	5.87E-08	3.72E-06
140 - 150 deg	3.97E-07	2.13E-06	1.06E-06	5.78E-08	3.65E-06
150 - 160 deg	3.88E-07	2.16E-06	1.08E-06	5.75E-08	3.68E-06
160 - 170 deg	3.75E-07	2.20E-06	1.11E-06	5.93E-08	3.74E-06
170 - 180 deg	3.68E-07	2.24E-06	1.11E-06	6.06E-08	3.78E-06
Full range:					
0 - 180 deg	4.30E-07	2.34E-06	1.13E-06	6.81E-08	3.97E-06

Neutron current relative to the corresponding averages included in the row "Full range: 0-180 deg" (in per cent)

Angle range	E<100 keV	100keV-1MeV	1MeV-10MeV	E>10 MeV	All
0 - 10 deg	90.97	104.28	105.32	159.37	104.08
10 - 20 deg	92.83	102.26	101.56	155.20	101.95
20 - 30 deg	96.23	99.80	97.53	137.57	99.41
30 - 40 deg	97.19	97.91	95.50	122.06	97.56
40 - 50 deg	99.54	98.75	96.76	118.86	98.62
50 - 60 deg	102.47	101.86	101.04	113.38	101.89
60 - 70 deg	104.90	103.28	103.90	107.04	103.69
70 - 80 deg	106.25	104.21	104.70	101.61	104.53
80 - 89 deg	102.12	104.92	102.83	95.31	103.86
89 - 91 deg	98.86	107.98	100.34	87.99	104.48
91 - 100 deg	101.90	103.80	101.94	88.35	102.80
100 - 110 deg	104.83	101.72	102.21	88.74	101.97
110 - 120 deg	102.77	99.82	100.69	87.65	100.18
120 - 130 deg	99.07	96.87	97.91	85.57	97.21
130 - 140 deg	95.62	92.67	95.21	86.14	93.60
140 - 150 deg	92.42	91.06	94.15	84.94	91.98
150 - 160 deg	90.27	92.00	95.41	84.50	92.65
160 - 170 deg	87.24	93.78	98.21	87.13	94.22
170 - 180 deg	85.75	95.46	98.54	88.97	95.18
0 - 180 deg	100.00	100.00	100.00	100.00	100.00

Table A1.4. Neutron current at R = 1 m from the target (see Fig. 1)

(in neutrons/cm^2/one beam electron)

Target diameter: **2.5** cm, Energy of the electron beam: **1.5** GeV

Total number of beam particles followed by FLUKA: 200000

	Neutrons				
Angle range	E<100 keV	100keV-1MeV	1MeV-10MeV	E>10 MeV	All
0 - 10 deg	1.76E-07	1.70E-06	9.73E-07	1.04E-07	2.95E-06
10 - 20 deg	1.89E-07	1.72E-06	9.70E-07	1.01E-07	2.98E-06
20 - 30 deg	2.17E-07	1.87E-06	1.05E-06	1.00E-07	3.23E-06
30 - 40 deg	2.52E-07	2.06E-06	1.17E-06	9.57E-08	3.58E-06
40 - 50 deg	2.83E-07	2.23E-06	1.25E-06	8.97E-08	3.85E-06
50 - 60 deg	3.09E-07	2.34E-06	1.30E-06	8.35E-08	4.04E-06
60 - 70 deg	3.28E-07	2.43E-06	1.34E-06	7.75E-08	4.17E-06
70 - 80 deg	3.36E-07	2.46E-06	1.35E-06	7.44E-08	4.22E-06
80 - 89 deg	3.37E-07	2.51E-06	1.33E-06	6.76E-08	4.25E-06
89 - 91 deg	3.36E-07	2.57E-06	1.32E-06	6.54E-08	4.29E-06
91 - 100 deg	3.37E-07	2.52E-06	1.33E-06	6.47E-08	4.24E-06
100 - 110 deg	3.36E-07	2.44E-06	1.34E-06	6.42E-08	4.17E-06
110 - 120 deg	3.26E-07	2.39E-06	1.31E-06	6.09E-08	4.09E-06
120 - 130 deg	3.05E-07	2.31E-06	1.27E-06	6.06E-08	3.94E-06
130 - 140 deg	2.75E-07	2.15E-06	1.21E-06	5.84E-08	3.70E-06
140 - 150 deg	2.46E-07	1.98E-06	1.13E-06	5.76E-08	3.42E-06
150 - 160 deg	2.10E-07	1.79E-06	1.04E-06	5.52E-08	3.10E-06
160 - 170 deg	1.81E-07	1.64E-06	9.76E-07	5.54E-08	2.85E-06
170 - 180 deg	1.56E-07	1.56E-06	9.56E-07	5.99E-08	2.73E-06
Full range:					
0 - 180 deg	2.96E-07	2.27E-06	1.25E-06	7.17E-08	3.89E-06

Neutron current relative to the corresponding averages included in the row "Full range: 0-180 deg" (in per cent)

	Neutrons				
Angle range	E<100 keV	100keV-1MeV	1MeV-10MeV	E>10 MeV	All
0 - 10 deg	59.53	74.85	77.82	144.67	75.92
10 - 20 deg	63.90	75.75	77.55	141.48	76.64
20 - 30 deg	73.29	82.18	83.75	139.83	83.07
30 - 40 deg	85.03	90.89	93.43	133.62	92.05
40 - 50 deg	95.62	98.12	99.60	125.13	98.90
50 - 60 deg	104.39	103.30	103.85	116.49	103.80
60 - 70 deg	110.50	106.96	106.79	108.12	107.20
70 - 80 deg	113.26	108.41	107.61	103.90	108.44
80 - 89 deg	113.71	110.71	106.28	94.35	109.21
89 - 91 deg	113.30	113.25	105.54	91.31	110.37
91 - 100 deg	113.59	110.82	106.04	90.29	109.11
100 - 110 deg	113.49	107.32	106.79	89.60	107.29
110 - 120 deg	109.80	105.24	104.82	84.99	105.08
120 - 130 deg	102.81	101.70	101.59	84.55	101.43
130 - 140 deg	92.77	94.92	96.84	81.47	95.13
140 - 150 deg	82.93	87.29	90.61	80.42	87.90
150 - 160 deg	70.95	78.84	83.39	77.06	79.67
160 - 170 deg	60.90	72.28	78.02	77.32	73.35
170 - 180 deg	52.68	68.69	76.48	83.53	70.25
0 - 180 deg	100.00	100.00	100.00	100.00	100.00

Table A2. Currents of other particles at R = 1 m from the target (see Fig. 1)

(in particles/cm^2/one beam electron)

Target diameter: **5** cm, Energy of the electron beam: **1.0** GeV

Total number of beam particles followed by FLUKA: 300000

	Produced particles				
Angle range	Protons	Pions+-	Photons	Electrons	Positrons
0 - 10 deg	3.97E-09	6.02E-09	6.87E-03	8.17E-05	6.20E-05
10 - 20 deg	3.03E-09	4.45E-09	2.52E-03	5.01E-05	3.35E-05
20 - 30 deg	2.45E-09	3.44E-09	1.38E-03	3.36E-05	2.07E-05
30 - 40 deg	1.90E-09	2.74E-09	8.79E-04	2.35E-05	1.31E-05
40 - 50 deg	1.64E-09	2.42E-09	6.44E-04	1.69E-05	8.65E-06
50 - 60 deg	1.54E-09	2.17E-09	5.04E-04	1.20E-05	5.50E-06
60 - 70 deg	1.44E-09	1.68E-09	4.05E-04	8.18E-06	3.43E-06
70 - 80 deg	1.38E-09	1.41E-09	3.30E-04	5.35E-06	2.03E-06
80 - 89 deg	1.16E-09	1.46E-09	2.96E-04	3.75E-06	1.27E-06
89 - 91 deg	9.69E-10	1.18E-09	2.27E-04	3.26E-06	1.20E-06
91 - 100 deg	1.18E-09	1.19E-09	2.47E-04	3.03E-06	1.03E-06
100 - 110 deg	1.35E-09	1.44E-09	1.89E-04	2.60E-06	6.80E-07
110 - 120 deg	1.66E-09	1.49E-09	1.58E-04	2.24E-06	5.26E-07
120 - 130 deg	2.18E-09	1.82E-09	1.37E-04	2.04E-06	4.11E-07
130 - 140 deg	2.72E-09	1.99E-09	1.26E-04	1.85E-06	3.35E-07
140 - 150 deg	3.41E-09	2.55E-09	1.23E-04	1.70E-06	2.85E-07
150 - 160 deg	3.53E-09	2.80E-09	1.26E-04	1.52E-06	2.29E-07
160 - 170 deg	3.56E-09	2.87E-09	1.30E-04	1.37E-06	2.02E-07
170 - 180 deg	4.32E-09	2.88E-09	1.32E-04	1.37E-06	1.96E-07
Full range:					
0 - 180 deg	1.91E-09	2.00E-09	4.46E-04	8.58E-06	4.39E-06

Current relative to the corresponding averages included in the row "Full range: 0-180 deg" (in per cent)

Angle range	Protons	Pions+-	Photons	Electrons	Positrons
0 - 10 deg	208.45	300.99	1539.44	951.98	1413.80
10 - 20 deg	158.90	222.55	563.95	583.48	762.59
20 - 30 deg	128.50	171.84	308.67	390.86	470.73
30 - 40 deg	99.56	136.89	197.06	274.08	298.54
40 - 50 deg	85.83	120.71	144.37	197.07	197.28
50 - 60 deg	80.93	108.39	113.05	140.00	125.33
60 - 70 deg	75.79	83.91	90.86	95.25	78.23
70 - 80 deg	72.37	70.27	73.90	62.38	46.27
80 - 89 deg	61.07	72.99	66.27	43.74	28.88
89 - 91 deg	50.85	58.87	50.86	38.03	27.41
91 - 100 deg	61.73	59.62	55.38	35.25	23.48
100 - 110 deg	70.90	72.03	42.44	30.33	15.51
110 - 120 deg	87.03	74.67	35.43	26.06	11.99
120 - 130 deg	114.32	90.76	30.67	23.74	9.36
130 - 140 deg	142.62	99.21	28.21	21.54	7.64
140 - 150 deg	178.96	127.62	27.65	19.84	6.50
150 - 160 deg	185.21	139.92	28.35	17.73	5.23
160 - 170 deg	186.69	143.23	29.18	15.95	4.60
170 - 180 deg	226.90	143.98	29.69	15.96	4.46
0 - 180 deg	100.00	100.00	100.00	100.00	100.00

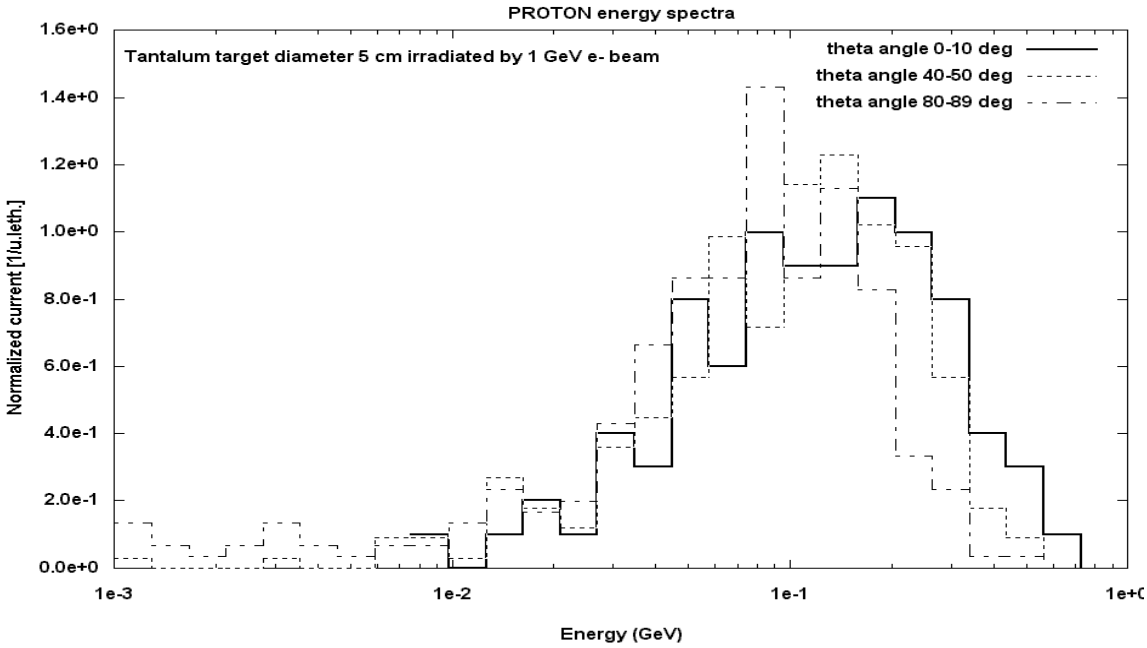

Fig. A3.1. Comparison of proton energy spectra at various ϑ angles.

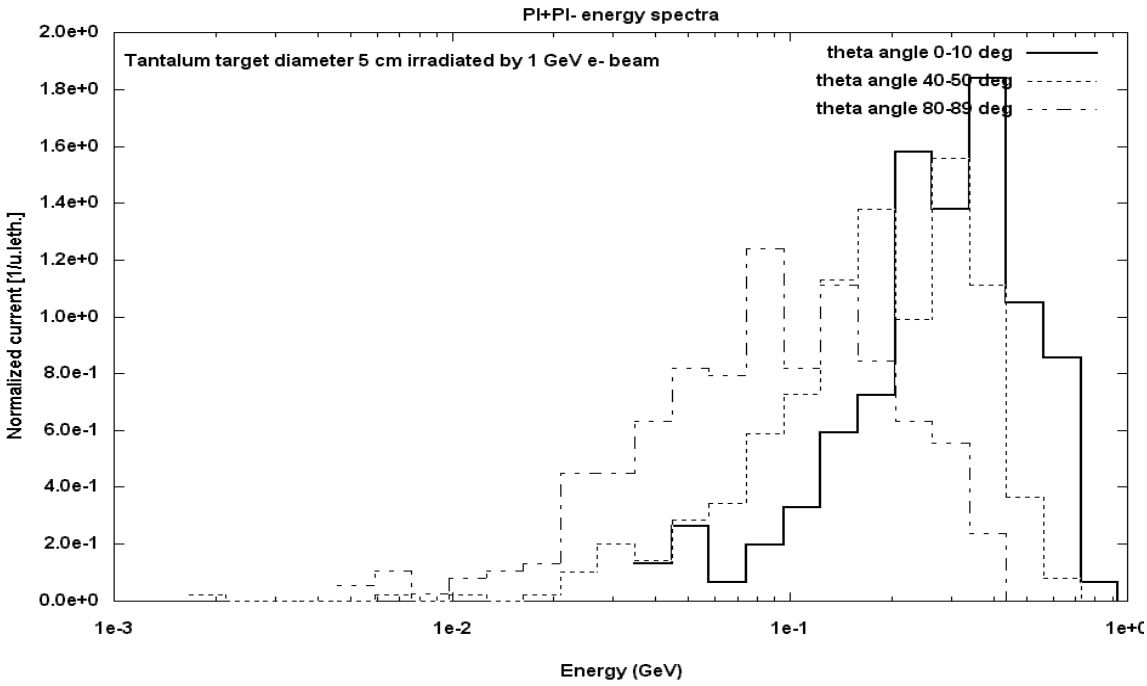

Fig. A3.2. Comparison of charged pion energy spectra at various ϑ angles.

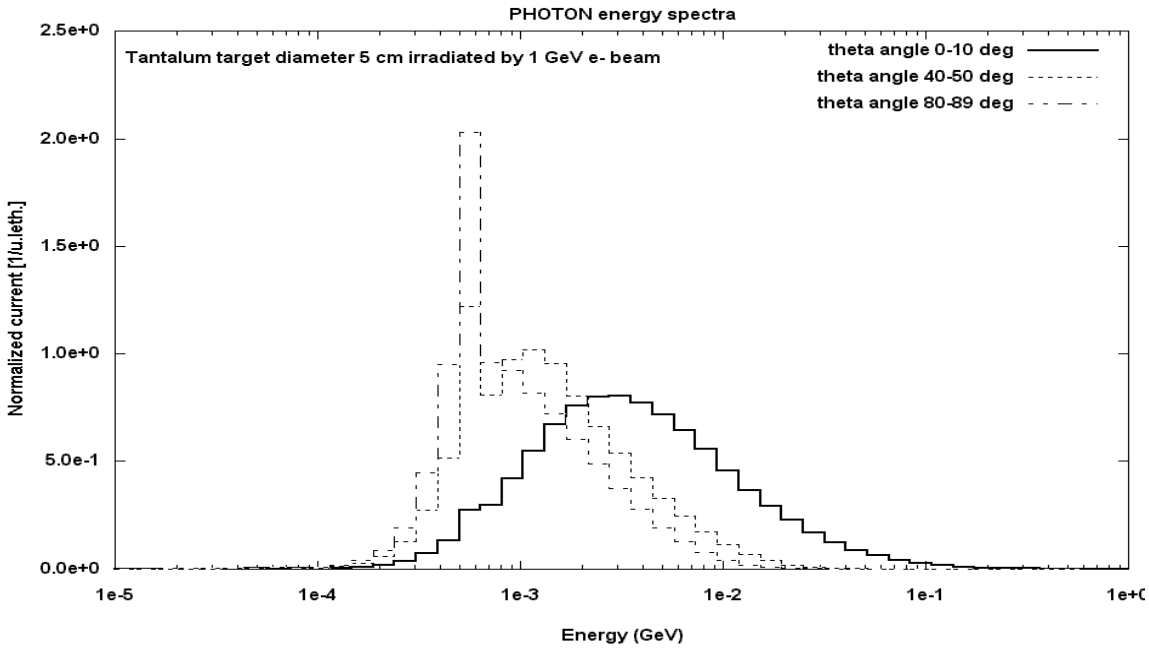

Fig. A3.3. Comparison of photon energy spectra at various ϑ angles.

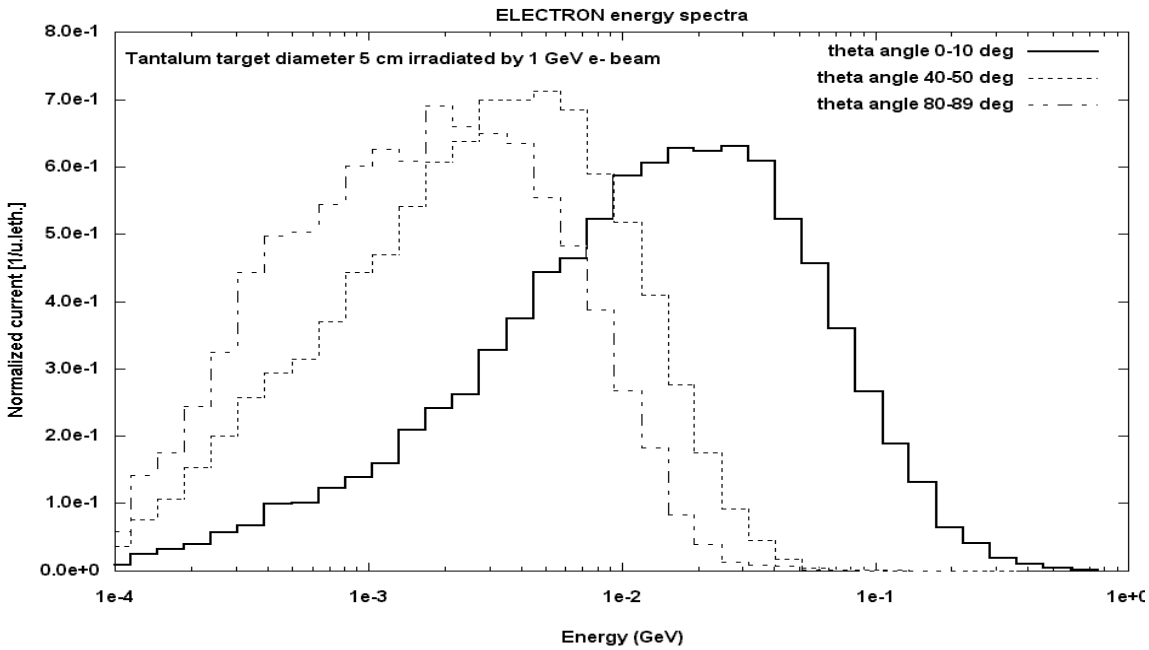

Fig. A3.4. Comparison of electron energy spectra at various ϑ angles.

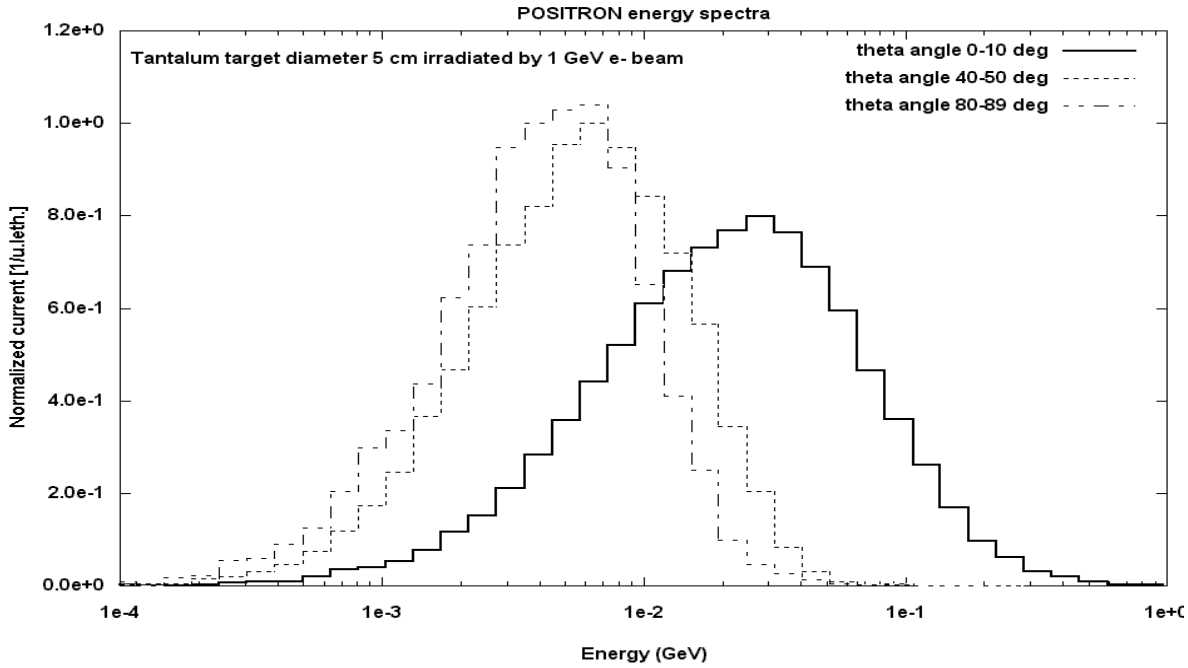

Fig. A3.5. Comparison of positron energy spectra at various ϑ angles.